Asian Journal of Research and Reports in Ophthalmology

3(3): 21-40, 2020; Article no.AJRROP.58544

Methods of Threshold Estimation (Algorithms) and New Techniques in Perimetry: A Review

Aristeidis Chandrinos[1*]

[1]*Department of Biomedical Sciences, School of Health Sciences, University of West Attica, Egaleo Park Campus, Athens, Greece.*

Author's contribution

Author designed, performed literature searches and analysis, and wrote the first draft of the manuscript. Author read and approved the final manuscript.

Article Information

Editor(s):
(1) Dr. Panagiotis Tsikripis, University of Athens, Greece.
Reviewers:
(1) S. Karthikeyan, Anna University, India.
(2) Terry Jacob, Mahatma Gandhi University, India.
Complete Peer review History: http://www.sdiarticle4.com/review-history/58544

Review Article

Received 27 April 2020
Accepted 01 July 2020
Published 14 July 2020

ABSTRACT

Recently, there have been several new developments in automated perimetry that have contributed to enhanced diagnosis and management of glaucoma. This paper will briefly review the classical algorithms of automated perimetry and also the latest advances in automated perimetry strategies, like SITA Faster algorithm. It will also explore the new algorithms for different perimeters and all the novel techniques, which has been shown to be a rapid, effective method of detecting glaucomatous visual field loss and have demonstrated the ability to predict the onset and progression of glaucomatous visual field deficits.

Keywords: Perimetry; glaucoma; algorithm; threshold; testing techniques.

1. INTRODUCTION

The technique used to determine the threshold sensitivity is called threshold algorithm (also named strategy). Normally, the visual threshold is described as a compilation of a frequency-of-seeing (FOS) curve, whereby the frequency of the percentage of seen responses (ordinate) is plotted as a function of the log of stimulus luminance (abscissa) and which

**Corresponding author: E-mail: achand@uniwa.gr;*

has a 50% probability of detection of repeated presentations [1-4]. This curve, illustrated in Fig. 1, is known as the psychometric frequency-of-seeing curve or FOS [5,6]. A frequency-of-seeing curve can be generated for each location in the visual field.

The curve, in general, has a sigmoid (S-shaped) appearance with a linear part in the middle [7]. The frequency of a 'seen' response is never 0% because of the presence of false-positive responses and never reaches 100% as a result of the presence of false-negative responses. Therefore, sufficiently dim stimuli will not be perceived, while sufficiently bright stimuli will. The boundary between perceptible and imperceptible stimuli is not sharply defined and spans approximately 3 decibels for trained observers [8].

The slope of the curve, as a measure of uncertainty in determining the threshold, is highly correlated to actual threshold or threshold deviation from age-appropriate normal values at a particular location and is an indication of the variability associated with the estimation of threshold. Consequently, a gradually flatter slope indicates increasing variability of the threshold estimate, whereas a progressively steeper slope indicates increasingly less variability [9].

The slope magnitude is also frequently described in terms of the inter-quartile range and more precisely the difference between the sensitivity values corresponding to the 25% and 75% seen responses. The magnitude of the variability is dependent upon a number of factors. It rises with age and rises with increase in eccentricity of the stimulus location, but it varies also among individuals of the same age [10,11].

In perimetry a conventional method for estimating the differential light threshold adjusts the stimulus luminance in small intervals or steps either in an ascending or a descending manner until it is perceived with a probability of 50%. This method, known as the method of limits, is time consuming when the initial stimulus luminance is far from the threshold.

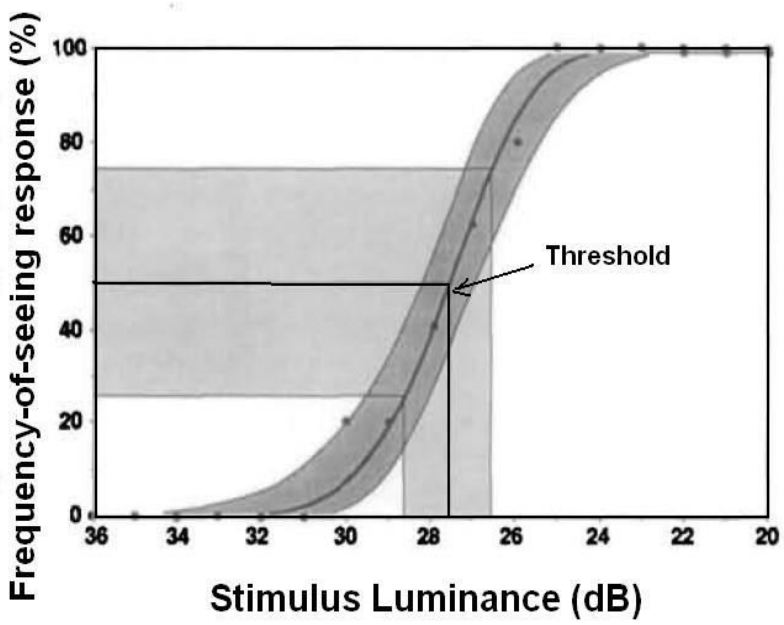

Fig. 1. The frequency-of-seeing curve

Percentage of seen response, (ordinate) is plotted as a function of stimulus luminance (abscissa) The data points represent the raw data; the solid line, the fitted curve; and the shaded area around the curve, the 95% confidence interval. The threshold is the stimulus intensity corresponding to 50% frequency-of-seeing. The light grey shaded area is the interquartile range, which is an estimate of the slope of the curve and frequency-of-seeing (by Chauhan et al., 1993)

Currently, an adaptive mode has been used. The stimulus luminance varies in ascending and descending steps, until the threshold is estimated. This process is also known as staircase or bracketing [12,13].

Generally in perimetry the commonly used algorithms utilize a double threshold crossing. If the initial stimulus is not seen, the luminance is increased in unit steps until a positive response is obtained. The stimulus luminance is then decreased in steps (which are half those used for the first estimation) until a negative response is obtained. The threshold is thereby crossed twice. The threshold can, of course, be approached from the opposite direction.

Wherever possible, the number of stimuli necessary to estimate the threshold is minimized with the intention of shortening the examination duration and thereby reducing the inherent variability in the threshold estimate arising from fatigue [14,15,16]. Of course, this specific variability decreases with increase in the number of threshold crossings, with smaller step size and increase in the number of estimations.

By and large, in the last 40 years automated perimetry has used an assortment of threshold algorithms. This variety of algorithms can be classified, depending upon their date of introduction into early, second generation and current algorithms. The second generation algorithms exhibit a reduction in examination duration, compared to that of the first invention, at the cost of some loss of accuracy of the threshold estimate whereas the current cohort of algorithms have employed advanced techniques taking advantage of increased computer processing speed to achieve a reduction in test duration without loss of accuracy in the threshold estimate.

2. THE EARLY ALGORITHMS

At late '70s, Octopus and Humphrey both adopted similar strategies for threshold estimation using the mean value of neighbouring stimulus locations combined with the slope of the age-corrected sensitivity gradient's data.

The Octopus series of perimeters initiate the examination at each of four 'principal' stimulus locations (termed anchor points) positioned near the centre of each quadrant of the visual field. The primary luminance of each stimulus is the age-corrected normal value minus 4dB. If patient gives a negative response, the following stimulus luminance is increased by 6dB. The examination continues by increasing the stimulus luminance in steps of 8dB until a positive patient's response is achieved. Subsequent to the threshold crossing, the stimulus luminance is reduced in steps of 4dB until the threshold is crossed for the second time. After the second crossing of threshold, the stimulus luminance is increased again in 2dB steps until the threshold is crossed for the third time. The last value is adjusted by 1dB in the reverse direction to the last response [17,18].

If the patient responds to the primary stimulus luminance positively, the luminance is decreased in steps of 2dB until a negative answer is achieved, after which the luminance is increased in 1dB steps until a positive reply again is gained. The estimated sensitivity at the four anchor points is applied to the former data of the slope of the age-corrected sensitivity gradient, to estimate the threshold of each of the nearby locations in the related quadrant.

The bracketing practice then continues in a similar fashion, in 4-2-1 dB steps. The primary luminance for the next set of following locations are calculated, in each case, from the median value of the three previously thresholded neighbouring localities and from the slope of the age-corrected sensitivity gradient [18,19].

On the other hand, the Humphrey Field Analyzer uses the Full Threshold algorithm to acquire a threshold estimate crossing twice each of four stimuli (termed seed points) situated 9° from both the horizontal and vertical meridians, correspondingly. Each one of these four seed points first luminance is 25dB and the threshold is crossed twice, in the order of 4dB and 2dB steps. The final 2dB crossing of threshold can take place in either an ascending or descending way. The threshold is calculated as the mean of the last positive and first negative patient's reply. The original value for the immediate neighbouring stimulus points, obtained from sensitivity data at the primary locations and of the slope of the hill of vision, is 2 dB brighter than the expected value [20,21].

3. SECOND-GENERATION ALGORITHMS

Through the decade of the '90s, Octopus and Humphrey implemented new algorithms in order to reduce the duration of an examination

that produces fatigue to the patient and consequently creates less accurate test results.

3.1 Dynamic Strategy

Octopus perimeters put into operation the Dynamic Strategy algorithm that is still currently in use, despite the algorithm no longer being up to date. Dynamic Strategy reduces the examination duration by 30-40% in areas of normal sensitivity and by 40-50% in areas of severe loss, compared with the Threshold algorithm [22,23].

The Dynamic Strategy algorithm uses luminance steps to adapt to the sensitivity at the specified stimulus location from data of the width of the FOS curve. When the visual field defect increases, then the step size increases too, from 2 dB to 10 dB, but threshold is crossed only once and the approximation is calculated as the mean of the two most recent stimulus luminances [22,24].

For sensitivities in the normal range, the Dynamic Strategy algorithm demonstrates lower variability between-examination than the Threshold algorithm. Conversely, the short-term fluctuation of the Dynamic Strategy is higher than the Threshold algorithm, but the long-term fluctuation is similar [25]. Obviously, the benefit of accuracy versus testing time is in favour of the Dynamic Strategy algorithm [22-25].

3.2 FASTPAC

The FASTPAC algorithm, introduced by Humphrey in 1991, applied a 3 dB step in either an ascending or a descending way correspondingly, and threshold is crossed only once [27]. A major effort in the development of new perimetric strategies is to find a reasonable trade-off between testing time and accuracy to minimize patient stress and simultaneously to improve reliability of results. A study by Glass and associates [28] in 1995, evaluated the properties of FASTPAC and compared FASTPAC to the standard 4-2 dB full-threshold procedure. Both procedures are staircase methods with predetermined step size for contrast variation. A variety of clinical studies that evaluated the practical capability of both strategies have given opposing results.

The FASTPAC algorithm examination time is approximately 35% shorter than the Full Threshold algorithms test period, but is at the cost of an approximately 25% increase in the short-term fluctuation (within-test variability) and an apparent underestimation of focal loss in glaucoma [28,29,30]. This focal loss underestimation, combined with the larger short-term fluctuation is influenced by the magnitude of the difference between the starting value and the measured threshold. A positive difference leads to an overestimation of threshold whilst a negative difference leads to an underestimation of the threshold; this outcome is more prominent for the FASTPAC algorithm than for the Full Threshold algorithm [28,30].

4. CURRENT ALGORITHMS

4.1 SITA Algorithms

The Swedish Interactive Threshold Algorithms (SITA) include two available algorithms: the SITA Standard, which is analogous to the Full Threshold algorithm, and the SITA Fast, which is analogous to the FASTPAC algorithm, both introduced in 1997 for SAP with the HFA [31-33].

The SITA algorithm was designed to reduce testing time, while still providing a sufficient test of visual sensitivity, in order to increase attention and result in a more reliable test. SITA Standard uses 4 dB and 2 dB steps and was designed to replace the Full Threshold program (e.g. Full Threshold 30-2), and SITA Fast uses a 4dB step only and was designed to replace FASTPAC, which is a simplified Threshold program [12,31].

Both algorithms reduce the examination duration in normal individuals: the SITA Standard algorithm is approximately 50% shorter compared to the Full Threshold algorithm, and the SITA Fast algorithm, 50% shorter compared to the FASTPAC algorithm. The SITA Fast algorithm is 41% shorter than the SITA Standard algorithm [21,32,34].

One may consider that a Full Threshold 30-2 visual field test on an eye, with significant pathology, might take 16 minutes to complete. The same test with SITA Standard would take about 8 minutes, and the same test with SITA Fast would take about 4.5 minutes. Running SITA with the 24-2 pattern instead of the 30-2 pattern can further reduce examination time. In addition, the 24-2 pattern gives adequate coverage for detecting and following

glaucomatous field defects. Both SITA algorithms make use of two Bayesian posterior probability functions (models) at each stimulus location. One function is a distribution of the probability of a seen response at any given value of sensitivity in the normal eye and the other function is a corresponding distribution in the glaucomatous eye [39,40]. The two probability models are based upon knowledge of the age-corrected threshold value, the between-individual variability in the estimation of threshold, the variation in the shape of the FOS curve between stimulus locations and the correlation of sensitivity between neighbouring stimulus locations. As the assessment continues each function is adjusted continuously (following the positive or negative response to each individual stimulus presentation), and the shape of each function repeatedly alters as the test progresses. The height of the function illustrates the most likely threshold at the given location and the width states the precision of the threshold estimation at any given moment in the examination [29,31,34].

The procedure of threshold estimation at any given location is ended when a predetermined level of accuracy is obtained, as predefined by the Error Related Factor (ERF) [31,35]. The balance between accuracy and test time stands for the magnitude of the ERF at each stimulus location. The estimation of threshold with the SITA Standard algorithm cannot be finished, without at least one crossing of the threshold. On the other hand, with the SITA Fast algorithm the threshold estimation can be terminated at any given location without a crossing of threshold [3,36], The subsequent inter-stimulus interval is based upon the individual response time window and the SITA algorithms determine the response time to each stimulus presentation.

Every response that take place within a 'listen time' window of 180 ms (which immediately follows the onset of the stimulus presentation), and also those which occur within a further 'listen time' window (which commences at a fixed time, after the response window and which runs into the 'listen window' related to subsequent stimulus) are designated as False Positive responses [31].

The entire response information obtained during the examination has been used to recalculate the approximate sensitivity at each stimulus location at the termination of the examination [31,36]. In particular, this procedure allows the estimated thresholds at the beginning of the examination to be recalculated from all available response information. The procedure also identifies and excludes those responses, which take place within the 'listen time' window (the false-positive responses), providing better assessment of threshold.

By applying this practice, the necessity for the traditional false-positive catch trials is also avoided and therefore a slight reduction in the examination time duration is allowed. Generally, the rate of the false-positive responses appears on the printout. But the response time of the patient can be affected by the magnitude of the stimulus luminance and the stimulus location and may vary during the examination [20,36]. The resulting threshold estimation achieved by either SITA algorithm signifies the stimulus luminance matching to a 50% probability on the FOS curve [3].

Taken as a whole, the SITA Standard and SITA Fast algorithms demonstrate good sensitivity and specificity for the detection of glaucomatous visual field loss, and involve a significant reduction in the examination duration, in comparison to the older algorithms [21,36,37]. However, the confidence limits for normality are greater for the SITA Fast algorithm than for the SITA Standard algorithm. The between-examination variability of the SITA Fast algorithm is also greater than that of the SITA Standard algorithm [20,45-47] The mean sensitivity in the normal eye is larger for both SITA algorithms, compared to the Full Threshold algorithm. In the glaucomatous population, both algorithms create a marginally higher mean sensitivity, compared to Full threshold and STATPAC algorithms but with a statistically deeper defect depth [21]. For sensitivities above 25 dB the SITA Standard algorithm illustrates better test- retest variability than Full Threshold, but below 25 dB the SITA Fast shows slightly poorer test-retest variability. In general, this improvement of test-retest variability is credited to the reduction in perimetric fatigue effect due to decreasing the test duration [20].

Some practitioners are not comfortable using SITA Fast as a standard field test for glaucoma. They prefer to use SITA Standard as the default test and use SITA Fast in special situations. The SITA Fast test can be utilized for patients to "learn" on. Once the patient is

comfortable with the testing procedure, it is better to switch to the SITA Standard test. The SITA Fast test can also be reserved for patients who cannot even tolerate the speed of the SITA Standard test. On the other hand, SITA algorithms cannot be used with the HFA 600 series due to the limited speed of the older processors and are only available for the HFA 700 series and later [38].

Recently, Heijl and associates (2019) introduced a new timesaving threshold visual field–testing strategy—Swedish Interactive Thresholding Algorithm (SITA) Faster, which is intended to replace SITA Fast [39]. According this clinical study, SITA Faster saved considerable test time. SITA Faster and SITA Fast gave almost identical results. There were small differences between SITA Faster and SITA Standard, of the same nature as previously shown for SITA Fast vs SITA Standard.

When designing SITA Fast, consequently the test was created to be less accurate than SITA Standard, and this was also revealed in clinical tests. Nevertheless, differences were small, and some investigators concluded that the shorter test was a pretty option in clinical practice and for screening.

Later results have shown that SITA Fast and SITA Standard are consistently effective for glaucoma detection, and analysis of a very large clinical perimetry database demonstrated that regardless of the fact that SITA Fast is to some extent less accurate in test points with poor sensitivity, this is not likely to make an ample difference in the time needed to detect progression [39].

On the other hand, SITA Faster necessitates only 1 reversal at prime test points instead of the 2 staircases used in earlier SITA tests. This is timesaving and reasonable because SITA Faster starts much closer to the expected threshold in the principal points.

Nonetheless, in SITA Faster, FN catch trials were discarded. While such trials have been generally used in computerized perimeters since the 1980s, it has been known for many years that FN rates depend more on visual field status than on the patient attention. Glaucoma eyes have much higher FN rates than normal eyes, and in patients with unilateral field loss FN responses are much more common in the defect eye, providing evidence that such responses are more suggestive of glaucomatous field loss than of patient consistency.

In SITA Faster, we have also abandoned the old rule that test point locations found to be perimetrically blind should be rechecked by presenting a second maximum intensity stimulus. One reason for making this change is the negative patient experience associated with not seeing the stimulus for long periods of time, which occurs in patients with eyes having severe field loss when using the older SITA strategies. It was noted in early pilot studies that patients with severe or end-stage glaucoma were those who noticed and appreciated SITA Faster the most.

This clinical study demonstrated a considerable reduction of test time with the SITA Faster algorithm compared with SITA Fast, which it was designed to replace (Table 1). With SITA Faster, the average test time was around 2 minutes in eyes with early glaucomatous field loss and sometimes shorter in normal fields. Test time depended considerably on the stage of glaucomatous field loss, however, and in eyes with advanced loss and VFI values <40% the test time was often twice as long—around 4 minutes for SITA Faster, while going down slightly in end-stage fields.

4.2 Zippy Adaptive Threshold Algorithm (ZATA)

In the 1980s a more efficient Bayesian approach was introduced to the methods of obtaining thresholds. One of the algorithms promoted [36] was called ZEST (Zippy Estimate by Sequential Testing). In the early 1990s the ZEST algorithm [12] was used to develop ZATA (Zippy Adaptive Threshold Algorithm).

Table 1. Test duration with SITA algorithms

Available as:	
SITA STANDARD (SS)	✓ Takes 7 min per eye
SITA FAST (SF)	✓ Takes 4 min per eye
SITA FASTER (SFr)	✓ Takes 2 min per eye

The Zippy Adaptive Threshold Algorithm (ZATA) was introduced for the Henson 8000 perimeter. Two versions of ZATA are available: Standard and Fast. Both algorithms use data from prior examinations to reduce the time for threshold estimation [37].

They follow the same philosophy as the SITA test in the HFA but integrate a number of important improvements that increase the speed of the test and the accuracy of its threshold estimates [13].

The first of these changes is that, when available, use is made of the findings from a previous test to set the starting intensity for each test location. This will reduce the number of presentations needed to find the threshold and hence speed up the test.

Alternatively, with the threshold algorithm the time taken to complete the test increases when there is a defect. This is because current threshold tests always start from normal age values rather than prior data. Using prior data not only speeds up the test it also results in a more accurate threshold estimate. It extends the concept behind the development of the SITA tests, which is to use as much prior data as possible to optimise the test [13,37].

The algorithm reduces the examination duration in normal eyes and in eyes with severe field loss. However, at the time of working on this review there are no any publications about the performance of these algorithms.

4.3 Tendency Oriented Perimetry (TOP)

The Tendency Oriented Perimetry (TOP) is a novel perimetric strategy, mainly designed to estimate the sensitivity of the visual field promptly, by using linear interpolation between test locations. TOP was initially introduced in 1996 for the Octopus perimeters [41].

This technique is based upon the correlation of sensitivity between neighbouring stimulus locations. A number of studies report that TOP is able to carry out accurate threshold determinations with a significantly reduced testing time [60].

Additionally, some studies have shown that TOP was four times faster than the traditional full-threshold technique and was successful in detecting visual field abnormalities. On the other hand, TOP produces an underestimation of sensitivity for small visual field deficits (one or two stimulus locations) and decreases the slope of the boundary around visual field deficits. Defects with TOP tended to be smaller, shallower, and with softer edges than with the standard approach [42].

The TOP algorithm uses a subject's response at a specified point, not only to estimate the sensitivity at that point, but also to modify the sensitivity approximation of surrounding points within the visual field [43]. Another previous study reported that association between mean deviation (MD) and loss variance (LV) for a conventional staircase procedure and the TOP algorithm were high, as assessed on a moderately sized group with mixed disease states [41,43].

In the TOP technique, the visual field is divided into four overlapping sub- matrices, such that, in the case of Program 32, each sub-matrix comprises 19 stimulus locations with a between-stimulus separation of 15°. Each matrix is then examined in sequential order. The cycle is repeated for all locations in each of the four sub-matrices and the estimated sensitivity is recorded. The final adjustment recalculates the estimates based upon the established approximations between adjacent locations [43].

4.4 German Adaptive Thresholding Estimation (GATE-i / GATE) Strategy

German Adaptive Thresholding Estimation (GATE) is a new, fast threshold strategy, which is comparable to the Full Threshold staircase and the SITA Standard strategy. The GATE-i algorithm is similar to the GATE algorithm. The only difference is in the reference field that is based upon the age-corrected normal values rather than upon the previously determined thresholds for the given individual [44].

The GATE-i algorithm starts by determining the sensitivity at each of five predefined seed locations. At every seed location the measured sensitivity is compared to the matching age-corrected normal value. Subsequently, the smallest deviation between the measured and age-corrected values of sensitivity is used to adjust the overall height of the expected visual field. The initial stimulus luminance at each subsequent stimulus location is slightly

decreased compared to the expected value. If the stimulus is 'seen', the luminance is reduced in 4 dB steps until a 'non-seen' response is obtained, after which the luminance is increased until a 'seen' response is obtained. If the initial luminance is 'not seen', the subsequent stimulus is presented at the maximum luminance. If the latter is 'not seen', the thresholding procedure is terminated at the given location. If the maximum luminance is 'seen', the subsequent stimulus is presented at 4 dB brighter than the initial presentation and the luminance is increased in 4 dB steps until a 'seen' response occurs. The stimulus is then presented 2 dB dimmer than the level at which the 'seen' response occurred. Therefore, the threshold is defined as the mean of the dimmest 'seen' stimulus and the brightest 'not seen' stimulus.

The characteristics of the threshold recorded with the GATE-i and GATE algorithms can be compared satisfactorily with those obtained with the Full Threshold algorithm, despite the fact that the examination duration is approximately half that of the Full Threshold strategy [44].

4.5 Continuous Light Increment Perimetry (CLIP)

The Continuous Light Increment Perimetry (CLIP) is a fast threshold strategy using stimuli with constantly rising luminance, offered for use with the Oculus Easyfield perimeter. In the CLIP algorithm, threshold value is assigned the moment the stimulus is perceived.

CLIP follows a completely different path compared to other mentioned algorithms. Quite the opposite of the regular bracketing methods, CLIP makes use of test points with stimulus luminance continuously increased in smaller steps (usually 1 dB), from an infrathreshold level according to the patient's reaction time until it is seen. Measuring the average reaction time of the patient and selecting the appropriate incremental rate of the luminance can achieve a considerable decrease of the examination time achieved, without losing accuracy or reproducibility.

CLIP demonstrates a higher Mean Sensitivity than the 4-2 dB algorithm of the Easyfield perimeter in individuals with glaucomatous field loss and tends to underestimate the depth of deep focal loss. Wabbels and colleagues study (2005) demonstrated that the examination duration for CLIP was 5.6 minutes for 55 stimulus locations, compared to 8.9 minutes for the 4-2 dB algorithm [58].

Capris et al., found that mean point-wise sensitivity difference in individuals with glaucomatous field loss between the SITA Fast and the Full Threshold (FT) algorithms of the Humphrey Field Analyzer (0.84 dB) was considerably lower than that found between CLIP and the 4-2 dB algorithm of the Easyfield perimeter and the Oculus FT strategy (1.71 dB). The mean test time duration for CLIP (450 $\pm$100 sec.) and for SITA Fast (366$\pm$72 sec.) was significantly shorter than the corresponding FT strategies [46].

Consequently, test duration for the CLIP algorithm is considerably shortened. Moreover, reproducibility of the results is increased. Additionally, a convenient side effect, patient's satisfaction level is kept high due to the fact that a stimulus with increasing luminance in the end is always observed. The CLIP algorithm has also been found suitable for the examination of children above the age of 8 years [47]. At the time of this review, no detailed descriptions of these algorithms have been published.

4.6 SPARK Precision and SPARK Quick

SPARK is the name of the strategy (and not a acronym) that was produced by the form of the stimuli during perimetry with the Oculus Easyfield perimeter. The SPARK Precision strategy is considered to be fast and reliable threshold perimetry and a suitable visual field test for glaucoma patients that can be performed in less or about 3 minutes per eye [48].

The large amounts of available statistical data make possible fast and very precise measurements of the threshold values in the central visual field. The inventive modular structure of the method in four different phases, allows an expanded use of the SPARK strategy in clinical practice.

The SPARK Quick strategy is for follow-up or for screening examinations. In patients with a prior visual field examination, the quality of the results is similar to those of the SPARK Precision algorithm [48] but with an additional decrease of examination duration of about 50%.

In this way the examination can be reduced to almost 1.5 minutes per eye.

SPARK also includes a training strategy to reduce the effect of the learning effects in standard perimetry, which lasts approximately 40 seconds. At the time of this review publishing no studies or publications are available about the performance of these algorithms against the more current established algorithms.

5. NOVEL TECHNIQUES OF PERIMETRY

Over the past 15 years, an accumulation of studies have recognized that extensive damage of the retinal ganglion cell axons (RGCs) happens prior to the appearance of visual field loss obtained by standard automated perimetry (SAP), at least when the last is expressed in dBs [49-52].

The first description for retinal ganglion cell loss, based upon histological proof, proposed that retinal ganglion cells with large diameter axons are preferentially damaged in early glaucoma [66,67]. Later, histological data from monkey eyes, illustrated that perimetry defects may be present in early glaucoma manifestation for minimal amounts of ganglion cell loss [52].

Retinal ganglion cells of dissimilar sizes have different physiologic purpose. Small cells that project to the parvocellular layers of the lateral geniculate body belong to the "P pathway" or the "colour system," while large cells that project to the magnocellular layers, belong to the "M pathway" or the "luminance system" [52]. Large optic nerve fibres selectively are lost in chronic human glaucoma [53].

A few years later, Johnson proposed that the idea of parallel M-cell and P-cell pathways is of clinical concern because of the likelihood that fussy eye diseases, like glaucoma, may preferentially affect one of these visual paths more than another, mainly in early phases of the disease development [34]. In that case it could be possible to use psychophysical tests to examine selectively particular vision functions, like motion or colour. Later, Johnson also introduced the " reduced redundancy hypothesis", as a substitute move towards the idea of early detection of functional defects [52,53].

Consequently, new methods has been developed to manipulate the "P pathway", like Short Wavelength Automated Perimetry (SWAP) or High-pass Resolution Perimetry (HRP), to control the "M pathway", such us Frequency Doubling Technology Perimetry (FDT) and Flicker Perimetry, to manage both "M and P pathways" like the Pulsar perimetry or by using minimum size of stimulus to avoid overlapping of ganglion cells receptive fields, such as Rarebit Perimetry (RBP).

5.1 Short Wavelength Automated Perimetry (SWAP)

Short Wavelength Automated Perimetry (SWAP) was used as a substitute technique, also known as "Blue on Yellow" perimetry that was developed to investigate K cell function in the 1980s and 1990s for the early identification of glaucomatous visual field loss [26,31,54].

SWAP is a type of visual field evaluation based on the approach that larger ganglion cells within the retina are selectively damaged throughout early glaucoma. Ten per cent of these larger ganglion cells belong to the blue-yellow pathway: part of the koniocellular pathway. The S cone system (short wavelength cones) are isolated by blue-yellow conditions of SWAP and the participation of other cone systems (red – long wavelength and green – medium wavelength) are reduced and the rods activity saturated through the adaptation to yellow light so that the blue stimuli are seen principally by the blue cone system [56].

Originally, clinicians considered that SWAP could reveal glaucomatous visual field loss earlier than that obtained by standard automated perimetry. This verification period of SWAP for the detection of defects prior to that identified by standard automated perimetry lasted for more than a decade and recently was reviewed in 2011, by Francis et al. [57].

The obvious disadvantage of SWAP over standard automated perimetry was the increased between-individual normal variability [26] and to the greater than before within- and between-examination variability for SWAP relative to standard automated perimetry, in normal individuals, in individuals with ocular hypertension and in individuals with open-angle glaucoma [58]. More recent research has not been able to confirm the early loss of visual field with SWAP or to monitor progression in more advanced cases of glaucoma [59].

On the contrary, SITA testing with standard white stimuli may detect just as much field loss in glaucoma as SWAP [32], or at least as early. A recent comparison study between SAP and SWAP, after 5 years follow up to OHT patients, demonstrated that both SAP and SWAP detected early glaucoma, with confirmation when visual field loss was evident. It appeared that each method identified early glaucoma in a subset of patients and these subsets overlapped only partially [58]. On the other hand, FDT matrix perimetry had a higher sensitivity for detecting glaucoma than did SWAP at a comparable level of specificity [55].

As a result of this high test-retest variability and the larger sensitivity to cataract, SWAP is no longer recommended for glaucoma management. In the future SWAP may instead find a place in maculopathy because during macula oedema the fluid primarily absorbs the blue light [60]. An evaluation study between standard automated perimetry (SAP) and short wavelength automated perimetry (SWAP) for the central 10-2 visual test procedure in patients with age-related macular degeneration (AMD) illustrated that although not all patients were suitable for SWAP examinations, it remains of ample value as a tool in research studies of visual loss in AMD [61,94].

5.2 High-pass Resolution Perimetry (HRP)

High-pass Resolution Perimetry (HRP) is used as an alternative perimetric technique developed to examine the "P" ganglion cell sampling density [60,64]. As expected, the HRP primarily mirrored the function of the P cells, as was the case for SAP [60]. It is well known that P cells representation in the central retina is much greater than in the periphery. Unlike SAP, HRP verifies sensitivity by varying the size and not by varying the luminance intensity of the stimulus. The HRP threshold is associated with retinal ganglion cell density as a function of eccentricity and of age [60].

The stimulus is a series of 'ring' target stimuli (Fig. 2) that mostly contain high spatial frequencies with dark borders (15 cdm^{-2}) surrounding a lighter center (25 cdm^{-2}), presented with duration of 165 ms [29]. The background luminance is 20 cdm^{-2}. The stimulus size is varied using an up-down staircase of variable steps over a range of 14 sizes of the stimulus, which changed with each stimulus being larger/ smaller than the previous stimulus by a factor of 1.26. The Ring program comprised 50 stimulus locations within the central visual field [60,64].

Table 2. SWAP Algorithm's pros and cons

Early detection of Glaucoma defects	Boring and tiring technique
Easy for follow-up progression	Test duration >20 min
Modify perimeters may perform	Lens opacities bias test results
Users well-known format	Refractive errors affect results
SITA makes it more easy	

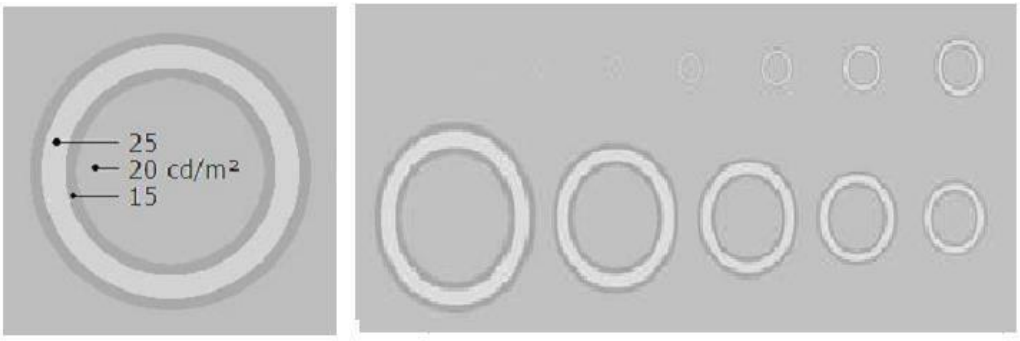

Fig. 2. High-pass resolution perimetry (HRP) test target

It consists of a bright circular core surrounded by dark borders. The dimensions and luminances are carefully calculated to make the target invisibly melt into the background if unresolved. Normal examination time is about 5 minutes. Fixation is monitored by occasionally projecting a target in the blind spot

The stimulus distribution of the HRP was thought to correspond with the arrangement of the ganglion cells. Therefore HRP could be superior to SAP in detection of visual field defects [85]. Nevertheless, such a theory suggests that HRP thresholds are sampling-limited. This latter suggestion has been disproved [64] on the basis that the true level of resolution acuity in the periphery is probably underestimated as a result of the proportionately higher contrast in the periphery. Therefore, an HRP threshold is unlikely to be a direct measure of the underlying ganglion cell density [62,63].

Furthermore, although a few studies concluded that the HRP performed better than SAP [6,60, 64] other investigators have found that HRP performed less well [65] or equally well [64,65].

The HRP demonstrates less variability at visual field locations with reduced sensitivity than does SAP [65]. The HRP may be associated with RNFL thickness and the neuro-retinal rim area. Although It continues to be used in its country of origin, Sweden [66-68], and used for vision rehabilitation and lesion management, it has never achieved extensive recognition elsewhere [69].

5.3 Rarebit Perimetry (RBP)

It is well known that Goldmann size III stimulus overlaps the visual field sampling, in a way that covers many ganglion cells receptive fields. As a consequence, the identification of abnormal function of any one fixed retinal ganglion cell is controlled, by those ganglion cells which remain functional and which produce normal receptive fields at the specified location of the stimulus.

An optional perimetric technique Rarebit Perimetry (RBP) was developed by utilizing a stimulus that presented a minimum of information (rare bits) with the purpose of locating very small spaces in the retinal neuronal matrix (Fig. 3) starting from dead (dysfunctional) or disconnected neurons [70]. Without a doubt, the stimuli used for RBP were to a large extent nearer in size to an individual ganglion cell receptive field in human [70,73].

The outcome of RBP was adversely affected by optical defocus [107] and by cataract [71,72]. RBP exhibited also a similar learning effect to SAP between the first and the second or third examination and with lower between-examination variability for five examinations over a five-week period than that for standard automated perimetry (SAP) for both stimulus size I and size III [73].

Previous reports have found central vision tests useful for macular lesions but their performance with lesions of the anterior visual pathways has not been explored. On the other hand, in various studies the rarebit test appeared highly capable of detecting optic neuropathies and chiasmal lesions and its simplicity and short test duration indicated a useful tool in screening settings [102]. Recently, a new computer-based quick test of neurovisual integrity was developed using segmented digits defined by rarebits, that is, receptive field –size bright dots briefly presented on a dark background [74].

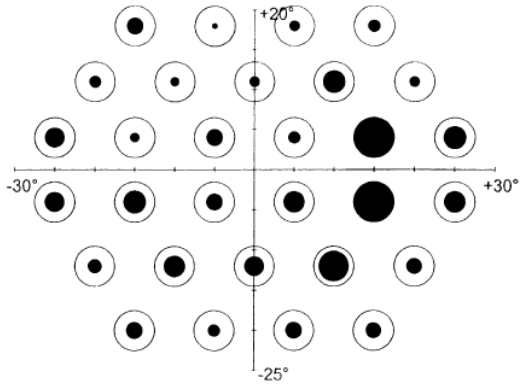

Fig. 3. Size and distribution of test areas in rarebit perimetry

Outer, open circles represent size of test areas. Inner, closed circles represent any missed probes, as the percentage of probes shown

5.4 Frequency-Doubling Technology Perimetry (FDT)

The frequency doubling phenomenon was first described by Kelly over 40 years ago as the "frequency-doubling illusion". Frequency Doubling Perimetry (FDP) originally was a psychophysical test that consisted of the presentation of low spatial frequency sinusoidal gratings (<1 cyc/deg) undergoing high temporal frequency counter-phase flicker at or above 15 Hz. Later versions of the Frequency Doubling Technology perimeter (Carl Zeiss Meditec, Inc., Dublin, CA), utilized a 0.25 cycles per degree sinusoidal grating, presented within a 10° x 10° stimulus square grid, which underwent counter phase flicker at 25Hz. Contrast was modulated until the grating was detected.

With such stimulus parameters, the grating appeared to exhibit twice the spatial frequency [74,75]. A second-generation version of the Frequency Doubling Technology perimeter, the Humphrey Matrix perimeter, utilizes a 0.5 cycles per degree sinusoidal grating, presented within a 5° x 5° stimulus patch, which undergoes counter phase flicker at 18 Hz [75]. The dynamic range of the device seems to be compatible with that of the FDT perimeter [75,76]. The age-corrected stimulus is presented at one of two contrasts, which should be seen by 95% and 99%, respectively (Fig.4), of the corresponding age-corrected normal population [38,77].

The frequency-doubling phenomenon is considered to be hindered by a subset (five per cent) of ganglion cells within the magnocellular pathway called My cells [78,79]. The My cells have larger diameter axons making them more prone to damage in early glaucoma [67]. Since the magnocellular ganglion cells are distributed differently from parvocellular, the visual field topography produced by FDP may again differ from that seen with SAP [79]. However, higher order cortical visual areas are also involved in the FDP processing [80].

Initially, it was recommended that the original FDT perimeter demonstrated a higher sensitivity and specificity for the detection of open angle glaucoma [38,81-83] compared to that of either SAP or SWAP. However, optical defocus and forward light scatter influence negatively the outcome of FDT perimetry [20]. Iester and colleagues have also been investigated the structure-function relationship for FDT and HRT, who found better correlation to SAP than to FDT [84]. More recent studies suggested that the outcome of the Humphrey Matrix perimeter is similar to that for SAP in the detection of glaucomatous abnormality [77,84-89], particularly for the detection of moderate to advanced visual field loss [87,90]. On the basis of these findings, despite the extensive literature, it is important to underline that the expected superiority of FDT to SAP remains unclear and FDT perimetry has not been yet substantiated as superior to the SAP gold standard [55,89,91,92].

5.5 Flicker Defined Form (FDF) Technology

Another current technology used in visual field examination is the Flicker Defined Form (FDF) stimulus [93], which stimulates the magnocellular pathway. The FDF stimulus creates an imaginary edge outline, which starts from a high temporal frequency driven imaginary stimulus based upon phase differences between the stimulus and the background [27,93]. The commercially available Heidelberg Edge Perimeter (FDF, Heidelberg Engineering, Germany) utilises that stimulus [94]. The test consists of flickering random dots on a background of 50 cdm^{-2} of mean luminance. The diameter of the imaginary stimulus is 5° and is created by a phase reversal of the black and white dots that flicker in counter phase to the background dots at a temporal frequency of 15Hz.

The visual field indices, Mean Deviation and Pattern Standard Deviation, for the Edge perimeter exhibit only a modest correlation with those derived by SAP using the Humphrey Visual Field Analyzer [18] for individuals with OAG [95]. The lack of agreement between the two types of perimetry may be explained by the presence of a considerable learning effect over three visits for the Edge stimulus [96]. On this basis, SAP is still the gold standard for detecting early glaucoma defects.

5.6 Pulsar Perimetry

Pulsar perimetry is a technique implied to evaluate both the parvocellular and the magnocellular visual pathways [97]. In this framework, the Pulsar perimeter evaluates the threshold of various visual functions, using high spatial and high temporal frequencies.

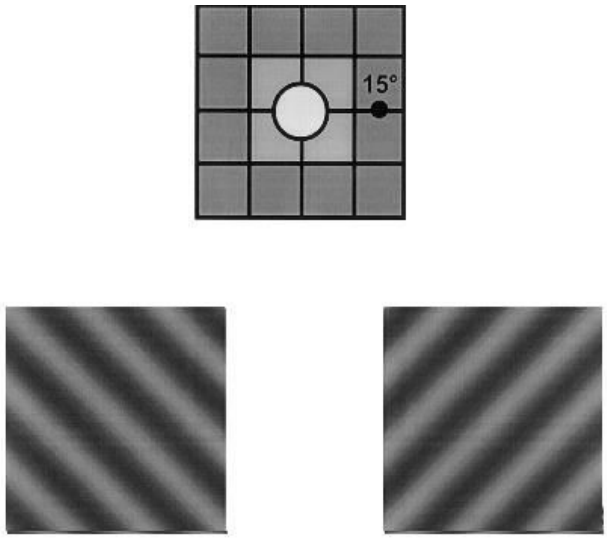

Fig. 4. Schematic illustration of the FDT stimulus
Top: The 17-location stimulus configuration in the commercial FDT perimeter. Bottom: Each stimulus has a 10° patch of sinusoidal grating oriented at 45° (right) or 135° (left)

The Pulsar stimulus consists of two images, the phase and counterphase image that alternate with a frequency of 10 Hz over 500ms and merge with the background luminance of 32 cd/m^2 at the edges to avoid stimulating direction-selective ganglion cells.

The Pulsar examination method of the Octopus 600 (Haag-Streit, 2014) exclusively uses the Tendency Oriented Perimetry (TOP) fast-threshold strategy, delivers fast and reliable results in the Octopus Program GP (Glaucoma, 59 test locations, central 30°) that can be completed within 2–4 minutes.

TOP is an algorithm, which in Pulsar perimetry takes into account the correlation of the threshold values in neighbouring locations and reduces the examination time by nearly 80% to just over two minutes, compared to 6–8 minutes in Dynamic strategy or 10–12 minutes in Normal strategy [98].

A number of studies demonstrated that Pulsar perimetry had greater sensitivity in the detection of early visual field loss in patients with OHT compared to SAP [97]. The between-examination variability was lower for Pulsar, compare6 to both standard automated perimetry (SAP) and FDT perimetry [98,99] and Pulsar perimetry seems able to detect more cases of clear progressive glaucomatous damage than either confocal scanning laser ophthalmoscopy or nerve fibre layer polarimetry [100].

Although Pulsar perimetry demonstrates greater sensitivity than FDT and shows advantages in early diagnosis of glaucoma, it has not yet achieved extensive recognition among the clinicians, and although it is still in use, it is probably misinterpreted [99].

5.7 Flicker Perimetry

Flicker perimetry consists of three different techniques, but all of them stimulate M ganglion cell function. These are: The Temporal Modulation perimetry (TMP), Luminance Pedestal Flicker perimetry (LPF) and Critical Flicker Fusion perimetry (CFF).

TMP computes the contrast thresholds for a permanent temporal frequency, for instance the minimum luminance at which a flickering stimulus of a given temporal frequency is perceived to demonstrate flicker [101]. However, TMP is supposed to distinguish glaucomatous defects earlier than standard automated perimetry, but the hypothesis is ambiguous. At 25Hz, TMP did not show any increased sensitivity, compared with SAP, in the detection of field loss in glaucoma suspect individuals or in those with OAG exhibiting recognized field loss by SAP [101]. Nevertheless, researchers, a long time ago

Table 3. Difficulties with threshold automated perimetry

✓ Boring and time-consuming
✓ Device not portable and not easy to detect progression
✓ Not easy for very young and for elderly people
✓ Significant learning effectand variability from test to test
✓ Not sensitive to early glaucoma
✓ Cataract or other media opacities bias results

recommended that TMP reveal considerably greater deformity in early glaucoma, at all temporal frequencies, and classified those cases of ocular hypertension that would develop glaucoma [85,91]. Individuals with normal visual function appeared to show a greater age-associated reduction in sensitivity for high temporal frequencies compared to low and medium temporal frequencies [101].

LPF perimetry demonstrates a flickering stimulus, superimposed on a base of a steady luminance, and specifies the temporal frequency required to separate the stimulus from the base [103]. The method is incorporated in the commercially available Medmont M600 perimeter (Medmont, Camberwell, Australia). Nonetheless, the clinical utility of LPF perimetry in patients with either OAG or OHT has not yet been investigated.

CFF perimetry determines the highest temporal frequency at which a flickering stimulus of constant luminance is originally perceived as a continuous (non- flickering) stimulus [104]. The literature is ambivalent as to whether the end point for CFF should be verified by increasing the temporal frequency until fusion is reported or by reducing the temporal frequency until flicker is perceived.

From a clinical point of view, different methods of flicker perimetry have been reported to detect retinal [105] and macular abnormalities [103,106]. Numerous studies have also reported that this method is superior to SAP in the investigation of glaucomatous field loss, although it has not become prevalent among investigators [107,108].

5.8 Moorfields Motion Displacement Test

A different current procedure, the motion detection threshold test (MDT) includes the presentation of a vertical bar of 85% Michelson contrast on a 10 cdm^{-2} white background at each of 32 stimulus locations [109]. Three fluctuations of 200 ms each alter the temporal location of each bar. Threshold is the detectable displacement perceived for 50% of the presentations.

Although MDT is a simple valuable test for the detection of glaucoma and is relatively resistant to the effects of intra-ocular light scatter [109,110], it still requires further comparative investigation.

6. CONCLUSIONS

Years ago, static threshold automated perimetry has been developed into an indispensable component in the successful detection and management of open angle glaucoma (OAG). Nonetheless, the length of the examination combined with the level of variability related to the measurement of perimetric sensitivity is becoming mismatched with the increasing financial and resource restrictions with health care provisions [110].

Recently, there have been several new developments in automated perimetry that have contributed to enhanced diagnosis and management of glaucoma. On one hand the SITA Faster algorithm development and simultaneously the Multifocal Electroretinogram (mfERG) and the Multifocal Visual Evoked Potential (mfVEP), which provide an objective measurement of the visual field may be the prosperous future for the perimetrists and vision practioners. Each of these techniques has presented distinct advantages for the diagnosis and management of glaucoma.

In conclusion, Wen and associates in their recent study (2019), using unfiltered real-world datasets of deep learning networks, show the ability to generate predictions for future visual field (VF) tests, given only a single VF [111]. Along with Ting and his partners (2019), future opportunities include training a neural network to identify the disc that would be associated with apparent VF loss across the range of disc size, as the current algorithms are very slow to detect the disease. Besides, deep learning could be used to detect

structural changes in optic nerve of progressive glaucoma [112].

Deep learning models may increase the speed of early diagnosis. Of course, they had more to improve and produce standards that will comply with the classical methods and techniques with more specificity to ophthalmologists. This may need more data collection of control healthy and glaucomatous patients, fatigue reduction and minimizing noise ratio associated with perimeters [112]. Artificial Intelligence may apply also for glaucoma detection on fundus photographs, by deep learning algorithms [113].

CONSENT

It is not applicable.

ETHICAL APPROVAL

It is not applicable.

COMPETING INTERESTS

Author has declared that no competing interests exist.

REFERENCES

1. Walsh JT. Neuro-ophthalmology: Clinical signs and symptoms. 4th Ed. Baltimore: Williams & Wilkins; 1978.
2. Chauhan BC, Mohandas RN, Whelan JH, McCormick TA. Comparison of reliability indices in conventional and high-pass resolution perimetry. Ophthalmology. 1993;100(7):1089-1094.
3. Bengtsson B, Heijl A. SITA Fast, a new rapid perimetric threshold test. Description of methods and evaluation in patients with manifest and suspect glaucoma. Acta Ophthalmol Scand. 1998;76(4):431-437.
4. Olsson J, Heijl A, Bengtsson B, Routzen H. Frequency-of-seeing in computerized perimetry. In: Mills RP. [Ed.] Perimetry Update 1992/1993. Amsterdam/New York: Kugler Publications. 551-556.
5. Bebie H, Fankhauser F, Spahr J. Static perimetry: Accuracy and fluctuations. Acta Ophthalmol (Copenh). 1976;54(3):339-348.
6. Acton JH, Bartlett NS, Greenstein VC. Comparing the Nidek MP-1 and Humphrey field analyzer in normal subjects. Optom Vis Sci. 2011;88(11):1288-97. DOI: 10.1097/ OPX 0b013e31822b3746 PMID: 21822159
7. Weber J, Rau S. The properties of perimetric thresholds in normal and glaucomatous eyes. Ger J Ophthalmol 1. 1992;2:79-85.
8. Drance MS, Anderson DR. Automatic Perimetry in glaucoma: A practical guide. New York: Grune & Stratton; 1985.
9. Walsh JT. Ophthalmology Monographs Vol. 3*:* Visual fields, examination and interpretation. New York: Oxford University Press; 2011.
10. Olsson J, Heijl A, Bengtsson B, Routzen H. Frequency-of-seeing in computerized perimetry: In: Mills RP, [Ed.] Perimetry Update 1992/1993. Amsterdam/New York: Kugler Publications 551-556.
11. Schiefer U, Põtzold J, Dannheim F. Conventional perimetry I: Introduction--basics. Ophthalmologe. 2005;102(6):627-644.
12. Turpin A, McKendrick AM, Johnson CA, Vingrys AJ. Properties of perimetric threshold estimates from full threshold, ZEST and SITA-like strategies, as determined by computer simulation. Invest Ophthalmol Vis Sci. 2003;44(11):4787-4795.
13. Denniss J, McKendrick AM, Turpin A. Towards patient-tailored perimetry: Automated perimetry can be improved by seeding procedures with patient-specific structural information. Transl Vis Sci Technol. 2013;2(4):3.
14. Hudson C, Wild JM, O'Neill EC. Fatigue effects during a single session of automated static threshold perimetry. Invest Ophthalmol Vis Sci. 1994;35(1):268-280.
15. Gonzalez de la Rosa M, Pareja A. Influence of the "fatigue effect" on the mean deviation measurement in perimetry. Eur J Ophthalmol. 1997;7(1):29-34.
16. Anderson AJ, McKendrick AM. Quantifying adaptation and fatigue effects in frequency doubling perimetry. Invest Ophthalmol Vis Sci. 2007;48(2):943-948.
17. Madea H, Nakamura M, Negri A. New perimetric threshold test algorithm with dynamic strategy and Tendency-Oriented Perimetry (TOP) in glaucomatous eyes. Eye. 2000;14:747-751.
18. Weijland A, Fankhauser F, Bebie H, Flammer J. “Automated Perimetry” - Visual Field Digest 05/06 Haag-Streit AG; 2004. ISBN 3-033-00108.

19. Zulauf M, Fehlmann P, Flammer J. Efficiency of the standard Octopus bracketing procedure compared to that of the 'Dynamic strategy' of Weber. In: Mills RP and Wall M, [Ed.] Perimetry Update 1994/95. Amsterdam/ New York: Kugler Publications. 1995;422-437.
20. Artes PH, Iwase A, Ohno Y, Kitazawa Y, Chauhan BC. Properties of perimetric threshold estimates from full threshold, SITA standard and SITA fast strategies. Invest Ophthalmol Vis Sci. 2002;43(8): 2654-2659.
21. Wild JM, Pacey IE, Hancock SA, Cunliffe IA. Between-algorithm, between-individual differences in normal perimetric sensitivity: Full threshold, FASTPAC and SITA. Swedish interactive threshold algorithm. Invest Ophthalmol Vis Sci. 1999;40(6): 1152-1161.
22. Weber J, Klimaschka T. Test time and efficiency of the dynamic strategy in glaucoma perimetry. Ger J Ophthalmol. 1995;4:25-31.
23. Anderson AJ, Johnson CA. Comparison of the ASA, MOBS and ZEST threshold methods. Vision Research. 2006;46(15): 2403-2411.
24. Johnson CA. Psychophysical factors that have been applied to clinical perimetry. Vision Res. 2013;90:25-31.
25. Zulauf MP, Fehlmann, Flammer J. Perimetry with normal Octopus technique and Weber 'dynamic' technique. Initial results with reference to reproducibility of measurements in glaucoma patients. Ophthalmologe. 1996;93(4):420-427.
26. Wild JM. Short wavelength automated perimetry. Acta Ophthalmol Scand. 2001;79(6):546-559.
27. Flanagan JG, Wild JM, Trope GE. Evaluation of FASTPAC, a new strategy for threshold estimation with the Humphrey field analyzer, in a glaucomatous population. Ophthalmology. 1993;100(6): 949-954.
28. Glass E, Schaumberger M, Lachenmayr BJ. Simulations for FASTPAC and the standard 4-2 dB full-threshold strategy of the Humphrey field analyzer. Invest Ophthalmol Vis Sci. 1995;36(9):1847-1854.
29. Wall M. What's new in perimetry. J Neuroophthalmol. 2004;24(1):46-55.
30. Barkana YE, Bakshi Y, Goldich Y, Morad A, Kaplan I, Avni, Zadok D. Characterization and comparison of the 10-2 SITA-standard and fast algorithms. Scientific World Journal. 2012;821802.
31. Johnson CA. Modern developments in clinical perimetry. Curr Opin Ophthalmol. 1993;4(2):7-13.
32. Bengtsson B, Heijl A. Diagnostic sensitivity of fast blue-yellow and standard automated perimetry in early glaucoma: A comparison between different test programs. Ophthalmology. 2006;113(7):1092-1097.
33. Punjabi OS, Lin SC, Stampe RL. Advances in mapping the glaucomatous visual field: from confrontation to multifocal visual evoked potentials. The Internet Journal of Ophthalmology and Visual Science. 2006;4(1).
34. Anderson DR, Patella VM. Automated static perimetry. Washington: CV Mosby; 1999.
35. Ng M, Racette L, Pascual JP, Liebmann JM, Girkin CA, Lovell SL, et al. Comparing the full-threshold and Swedish interactive thresholding algorithms for short-wavelength automated perimetry. Invest Ophthalmol Vis Sci. 2009;50(4):1726-33.
36. Johnson CA, Wall M, Thompson HS. A history of perimetry and visual field testing. Optom Vis Sci. 2011;88(1):E8-15.
37. Budenz DL, Rhee P, Feuer WJ, McSoley J, Johnson CA, Anderson DR. Comparison of glaucomatous visual field defects using standard full threshold and Swedish interactive threshold algorithms. Archives of Ophthalmology. 2002;120(9):1136–1141.
38. Johnson CA, Samuels SJ. Screening for glaucomatous visual field loss with frequency-doubling perimetry. Invest Ophthalmol Vis Sci. 1997;38(2):413-425.
39. Heijl A, Patella VM, Chong LX, et al. A new SITA perimetric threshold testing algorithm: Construction and a multicenter clinical study. Am J Ophthalmol. 2019;198: 154-165.
40. Henson DB, Emuh T. Monitoring vigilance during perimetry by using pupillography. Invest Ophthalmol Vis Sci. 2010;51(7): 3540-3543.
41. Scherrer M, Fleischhauer JC, Helbig H, Johann Auf der Heide K, Sutter FK. Comparison of tendency-oriented perimetry and dynamic strategy in octopus perimetry as a screening tool in a clinical setting: A prospective study. Klin Monbl Augenheilkd. 2007;224(4):252-254.
42. Morales J, Weitzman ML, Gonzɑlez de la Rosa M. Comparison between Tendency-

Oriented Perimetry (TOP) and octopus threshold perimetry. Ophthalmology. 2000;107(1):134-142.
43. Anderson AJ. Spatial resolution of the tendency-oriented perimetry algorithm. Invest Ophthalmol Vis Sci. 2003;44(5): 1962-1968.
44. Schiefer U, Pascual JP, Edmunds B, Feudner E, Hoffmann EM, Johnson CA, et al. Comparison of the new perimetric GATE strategy with conventional fullthreshold and SITA standard strategies. Invest Ophthalmol Vis Sci. 2009;50(1): 488-494.
45. Wabbels BK, Diehm S, Kolling G. Continuous light increment perimetry compared to full threshold strategy in glaucoma. Eur J Ophthalmol. 2005;15(6): 722-729.
46. Capris P, Autuori S, Capris E, Papadia M. Evaluation of threshold estimation and learning effect of two perimetric strategies, SITA Fast and CLIP, in damaged visual fields. Eur J Ophthalmol. 2008;18(2):182-190.
47. Wabbels BK, Wilscher S. Feasibility and outcome of automated static perimetry in children using continuous light increment perimetry (CLIP) and fast threshold strategy. Acta Ophthalmol Scand. 2005;83(6):664-669.
48. Gonzalez de la Rosa M, Gonzalez-Hernandez M, Sanchez-Garcia M, Rodriguez de la Vega R, Diaz-Aleman T, Pareja Rios A. Oculus-Spark perimetry compared with 3 procedures of glaucoma morphologic analysis (GDx, HRT and OCT). Eur J Ophthalmol. 2013;23(3):316-323.
49. Harwerth RS, Carter-Dawson L, Smith EL, Barnes G, Holt WF, Crawford MLJ. Neural losses correlated with visual losses in clinical perimetry. Investigative Ophthalmology and Visual Science. 2004;45:3152-3160.
50. Malik R, Swanson WH, Garway-Heath DF. Structure-function relationship' in glaucoma: Past thinking and current concepts. Clin Exp Ophthalmol. 2012;40(4):369-380.
51. Medeiros FA, Lisboa R, Weinreb RN, Girkin CA, Liebmann JM, Zangwill LM. A combined index of structure and function for staging glaucomatous damage. Arch Ophthalmol. 2012;130(9):1107-1116.
52. Medeiros FA, Zangwill LM, Bowd C, Mansouri K, Weinreb RN. The structure and function relationship in glaucoma: Implications for detection of progression and measurement of rates of change. Invest Ophthalmol Vis Sci. 2012;53(11): 6939-6946.
53. Wang Y, Xu K, Zhang H, Zhao J, Zhu X, Wang Y, Wu R. Retinal ganglion cell death is triggered by paraptosis via reactive oxygen species production: A brief literature review presenting a novel hypothesis in glaucoma pathology. Molecular Medicine Reports. 2014;10: 1179-1183.
54. Havvas I, Papaconstantinou D, Moschos MM, Theodossiadis PG, Andreanos V, Ekatomatis P, Vergados I, Andreanos D. Comparison of SWAP and SAP on the point of glaucoma conversion. Clin Ophthalmol. 2013;7:1805-1810.
55. McBride J, Rowe FJ. Review of the use of SWAP and FDT for the early detection of visual field loss. Ophthalmology Research: An International Journal. 2014;78-95.
56. Heijl A, Bengtsson B, Patella A. Effective perimetry. Zeiss Visual Field Primer, 4th Edition; 2012.
57. Francis BA, Singh K, Lin SC, Hodapp E, Jampel HD, Samples JR, Smith SD. Novel glaucoma procedures: A report by the American Academy of Ophthalmology. Ophthalmology. 2011;118(7):1466-1480.
58. Blumenthal EZ, Sample PA, Berry CC, Lee AC, Girkin CA, Zangwill L, Caprioli J, Weinreb RN. Evaluating several sources of variability for standard and SWAP visual fields in glaucoma patients, suspects and normals. Ophthalmology. 2003;110(10): 1895-1902.
59. Alencar LM, Medeiros FA. The role of standard automated perimetry and newer functional methods for glaucoma diagnosis and follow-up. Indian J Ophthalmol. 2011;59(Suppl):S53-58.
60. Chandrinos A. Aspects of perimetric learning index. PhD Thesis, Cardiff University, Wales, UK; 2017.
61. Acton JH, Gibson JM, Cubbidge RP. Quantification of visual field loss in agerelated macular degeneration. PLoS One. 2012;7(6):e39944.
62. Frisın L. High-pass resolution perimetry. A clinical review. Doc Ophthalmol. 1993;83(1):1-25.
63. Frisen L, Nikolajeff F. Properties of high-pass resolution perimetry targets. Acta Ophthalmol (Copenh). 1993;71(3):320-326.

64. Ennis FA, Johnson CA. Are high-pass resolution perimetry thresholds sampling limited or optically limited? Optom Vis Sci. 2002;79(8):506-511.
65. Artes PH, Chauhan BC. Longitudinal changes in the visual field and optic disc in glaucoma. Prog Retin Eye Res. 2005;24(3):333-354.
66. Kalaboukhova L, Fridhammar V, Lindblom B. Glaucoma follow-up by the Heidelberg retina tomograph--new graphical analysis of optic disc topography changes. Graefes Arch Clin Exp Ophthalmol. 2006;244(6): 654-662.
67. Martin LM, Nilsson AL. Rarebit perimetry and optic disk topography in pediatric glaucoma. J Pediatr Ophthalmol Strabismus. 2007;44(4):223-231.
68. Frisen L, Jensen C. How robust is the optic chiasm? Perimetric and neuro-imaging correlations. Acta Neurol Scand. 2008; 117(3):198-204.
69. Sabel BA, Henrich-Noack P, Fedorov A, Gall C. Vision restoration after brain and retina damage: The "residual vision activation theory". Prog Brain Res. 2011;192:199-262.
70. Hackett DA, Anderson AJ. Determining mechanisms of visual loss in glaucoma using Rarebit perimetry. Optom Vis Sci. 2011;88(1):48-55.
71. Salvetat ML, Zeppieri M, Parisi L, Brusini P. Rarebit perimetry in normal subjects: Test-retest variability, learning effect, normative range, influence of optical defocus and cataract extraction. Invest Ophthalmol Vis Sci. 2007;48(11):5320-5331.
72. Nilsson MO, Abdiu CG, Laurell, Martin L. Rarebit perimetry and fovea test before and after cataract surgery. Acta Ophthalmol. 2010;88(4):479-482.
73. Vislisel JM, Doyle CK, Johnson CA, Wall M. Variability of rarebit and standard perimetry sizes I and III in normals. Optom Vis Sci. 2011;88(5):635-639.
74. Frisen L. Rapid assessment of neurovisual integrity using multiple rarebits. Ophthalmology. 2013;120(9):1756-1760.
75. Anderson AJ, Johnson CA, Fingeret M, Keltner JL, Spry PG, Wall M, Werner JS. Characteristics of the normative database for the Humphrey matrix perimeter. Invest Ophthalmol Vis Sci. 2005;6(4):1540-1548.
76. Artes PH, Hutchison DM, Nicolela MT, LeBlanc RP, Chauhan BC. Threshold and variability properties of matrix frequency-doubling technology and standard automated perimetry in glaucoma. Invest Ophthalmol Vis Sci. 2005;6(7):2451-2457.
77. Johnson C. Chapter 9: Detecting functional changes in the Patient's vision: Visual field analysis. Clinical Glaucoma Care Ed. Samples J & Schacknow P, Springer; 2008. SBN-978-1-4614-4171-7.
78. Hood DC, Kardon RH. A framework for comparing structural and functional measures of glaucomatous damage. Progress in Retinal and Eye Research. 2007;26:688-710.
79. Anderson AJ, Johnson CA. Mechanisms isolated by frequency-doubling technology perimetry. Invest Ophthalmol Vis Sci. 2002;43:388-401.
80. Zeppieri M, Demirel S, Kent K, Johnson CA. Perceived spatial frequency of sinusoidal gratings. Optom Vis Sci. 2008;85(5):318-329.
81. Casson EJ, James B, Rubinstein A, Haggai A. Clinical comparison of frequency doubling technology perimetry and Humphrey perimetry. Br J Ophthalmol. 2000;85:360–362.
82. Horn FK, Scharch V, Mardin CY, Lämmer R, Kremers J. Comparison of frequency doubling and flicker defined form perimetry in early glaucoma. Graefes Arch Clin Exp Ophthalmol. 2016;254(5):937-46.
83. Cello KE, Nelson-Quigg JM, Johnson CA. Frequency doubling technology perimetry for detection of glaucomatous visual field loss. Am J Ophthalmol. 2000;129(3):314-322.
84. Iester M, Perdicchi A, Capris E, Siniscalco A, Calabria, Recupero SM. Comparison between discriminant analysis models and 'Glaucoma Probability Score' for the detection of glaucomatous optic nerve head changes. J Glaucoma. 2008;17:535-540.
85. Spry PG, Johnson CA, SL M, Cioffi GA. Psychophysical investigation of ganglion cell loss in early glaucoma. J Glaucoma. 2005;14:11-19.
86. Brusini P, Salvetat ML, Parisi L, Zeppieri M. Probing glaucoma visual damage by rarebit perimetry. Br J Ophthalmol. 2005;89:180-184.
DOI: 10.1136/bjo
87. Hong S, Na K, Kim CY, Seong GJ. Learning effect of Humphrey matrix perimetry. Can J Ophthalmol. 2007;42: 707-711.

88. Racette L, Tafreshi A, Liebmann JM, Girkin CA, Lalezary M, Zangwill LM, Weinreb RN, Sample PA. Visual function specific perimetry to identify glaucomatous visual loss using three different definitions of visual field abnormality. Investigative Ophthalmology & Visual Science. 2008;49: 1157.
89. Redmond T, O'Leary N, Hutchison DM, Nicolela MT, Artes PH, Chauhan BC. Visual field progression with frequency-doubling matrix perimetry and standard automated perimetry in patients with glaucoma and in healthy controls. JAMA Ophthalmol. 2013;131(12):1565-72.
90. Burgansky-Eliash Z, Wollstein G, Patel A, Bilonick RA, Ishikawa H, Kagemann L, et al. Glaucoma detection with matrix and standard achromatic perimetry. Br J Ophthalmol. 2007;91(7):933-938.
91. Wang X, Xu K, Zhang H, Zhao J, Zhu X, Wang Y, Wu R. Retinal ganglion cell death is triggered by paraptosis via reactive oxygen species production: A brief literature review presenting a novel hypothesis in glaucoma pathology. Molecular Medicine Reports. 2014;10: 1179-1183.
92. Lamparter J, Russel RA, Schulze A, Schuff AC, Pfeiffer N, Hoffmann E. Structure-function relationship between FDF, FDT, SAP and scanning laser ophthalmoscopy in glaucoma patients. Invest Ophthalmol Vis Sci. 2012;53(12):7553-9.
93. Horn FK, Scharch V, Mardin CY, et al. Comparison of frequency doubling and flicker defined form perimetry in early glaucoma. Graefes Arch Clin Exp Ophthalmol. 2016;254:937–946.
94. Perez CA, Ferreras A, Le Pablo, Pajarin AB, Polo V. Relationship between the automated classification of Heidelberg retina tomograph and main indices of short-wavelength automated perimetry. Acta Ophthalmologica. 2010;87.
95. Perez CA, Gil-Arribas L, Ferreras A, Otin S, Altemir I, Fernadez S, Julvez IP, Fuertes I. Relationship between flicker FDF perimetry and standard automated perimetry. Acta Ophthalmologica. 2010;88.
96. Lamparter J, Schulze A, Schuff AC, Pfeiffer N, Hoffmann EN. Learning curve of flicker defined form perimetry. Investigative Ophthalmology & Visual Science. 2010;51.
97. Gonzalez-Hernandez M, Garcia-Feijoo J, Sanchez Mendez M, Gonzalez de la Rosa M. Combined spatial, contrast and temporal functions perimetry in mild glaucoma and ocular hypertension. Eur J Ophthalmol. 2004;14:514–522.
98. Gonzalez de la Rosa G, Hernandez G, Estevez A, Aleman D, Plasencia A. Diagnostic capability of pulsar, FDT and HRT-II in glaucoma suspects. Arch Soc Esp Oftalmol. 2007;82:413-422.
99. Gonzalez de la Rosa M, Gonzalez-Hernandez M, Garcia-Feijoo J, et al. Comparacion del rango de medida de defectos entre la perimetria estandar blanco/blanco y la perimetria Pulsar. Arch Soc Esp Oftalmol. 2011;86:113–117.
100. Gonzalez de la Rosa M, Gonzalez-Hernandez M, Diaz-Aleman T. Linear regression analysis of the cumulative defect curve by sectors and other criteria of glaucomatous visual field progression. Eur J Ophthalmol. 2009;19:416–424.
101. Eisen-Enosh A, Farah N, Burgansky-Eliash Z, et al. Evaluation of critical flicker-fusion frequency measurement methods for the investigation of visual temporal resolution. Sci Rep. 2017;7:15621.
102. Hirasawa K, Shoji N, Kasahara M, et al. Comparison of size modulation and conventional standard automated perimetry with the 24-2 test protocol in glaucoma patients. Sci Rep. 2016;6: 25563.
103. Bernardi Luciana, Costa P. Vital and ineu Oto Shi Flicker perimetry in healthy subjects: Influence of age and gender, learning effect and short-term fluctuation. Arq Bras Oftalmol. 2007;70(1):91-9.
104. Roberti G, Manni G, Riva I, et al. Detection of central visual field defects in early glaucomatous eyes: Comparison of humphrey and octopus perimetry. PLoS One. 2017;12(10):e0186793.
105. Stavrou EP, Wood JM. Central visual field changes using flicker perimetry in type 2 diabetes mellitus. Acta Ophthalmologica Scandinavica. 2005;83:574-580.
106. Phipps JA, Dang TM, Vingrys AJ, Guymer RH. Flicker perimetry losses in age-related macular degeneration. Investigative Ophthalmology and Visual Science. 2004;45:3355-3360.
107. Matsumoto C, Takada S, Okuyama S, Arimura E, Hashimoto S, Shimomura Y. Automated flicker perimetry in glaucoma using Octopus 311: A comparative study with the Humphrey matrix. Acta

Ophthalmologica Scandinavica. 2006;84: 210-215.
108. Turpin A, Artes PH, McKendrick AM. The open perimetry interface: An enabling tool for clinical visual psychophysics. Journal of Vision. 2012;12:22.
109. Oleszczuk JD, Bergin C, Sharkawi E. Comparative resilience of clinical perimetric tests to induced levels of intraocular straylight. Investigative Ophthalmology and Visual Science. 2012;53:1219-1224.
110. Bergin C, Redmond T, Nathwani N, Verdon-Roe GM, Crabb DP, Anderson RS, Garway-Heath DF. The effect of induced intraocular straylight on perimetric tests. Invest Ophthalmol Vis Sci. 2011;52(6): 3676-3682.
111. Wen JC, Lee CS, Keane PA, Xiao S, Rokem AS, Chen PP, et al. Forecasting future Humphrey visual fields using deep learning. PLoS ONE. 2019.;14(4): e0214875.
112. Ting DSW, Pasquale LR, Peng L, et al. Artificial intelligence and deep learning in ophthalmology. Br J Ophthalmol. 2019;103:167–175.
113. Jammal AA, Thompson AC, Mariottoni EB, et al. Human versus machine: Deep learning algorithm to human gratings for detecting glaucoma in fundus. Photographs Ophthalmol. 2020;211:123–131.

Peer-review history:
The peer review history for this paper can be accessed here:
http://www.sdiarticle4.com/review-history/58544